Three-photon holographic microscopy for deep precise optogenetics

Supplementary information

Aysha S. Mohamed Lafirdeen[1†], Cécile Telliez[1,6†], Jérémie Nataf[1], Thi Phuong Lien Ung[1,7], Rafael Castillo-Negrete[1], Hassan Heidarisaani[1], Benoît C. Forget[1], Antonia Drinnenberg[2], Charu Ramakrishnan[2], La'Akea Siverts[3], Tanya L. Daigle[3], Bosiljka Tasic[3], Hongkui Zeng[3], Karl Deisseroth[2,4,5], Emiliano Ronzitti[1], Christiane Grimm[1,8], Valeria Zampini[1], Eirini Papagiakoumou[1]*, Valentina Emiliani[1]*

[1] Institut de la Vision, Sorbonne Université, INSERM, CNRS, F-75012 Paris, France
[2] Department of Bioengineering, Stanford University, Stanford, CA 94305, USA
[3] Allen Institute for Brain Science, Seattle, WA, USA
[4] Howard Hughes Medical Institute, Stanford University, Stanford, CA 94305, USA
[5] Department of Psychiatry and Behavioral Sciences, Stanford University, Stanford, CA 18 94305, USA

[6] Current affiliation: Laboratory of Neural Circuit Dynamics, Brain Research Institute, University of Zurich, Zurich, Switzerland

[7] Current affiliation: Innovation instrument, Essilor International, 39-69 Bd Jean Baptiste Oudry, 94000 Créteil, France

[8] Current affiliation: Multiscale Bioimaging Cluster of Excellence, University Medical Center Göttingen, Göttingen, Germany

*Correspondance : eirini.papagiakoumou@inserm.fr; valentina.emiliani@inserm.fr

†These authors contributed equally.

Table of Contents

Supplementary Table 1: Optical configurations for 3P excitation under TF-CGH illumination.

Wavelength (nm)	f_0	$f_{0'}$	f_1	f_2	f_3	f_4	f_5	f_6	Objective	FWHMz of a 12-15 µm spot (µm)
	(mm)									
1300	-	-	-150	750	400	200	500	500	Olympus 25x	13.2±1.7 (n=4)
1300	-	-	-150	400	400	400	400	200	Nikon 40x	5.1±0.3 (n=10)
1700	150	150	-150	750	400	200	500	500	Olympus 25x	18.1±1.7 (n=5)
1700	150	150	-150	400	200	200	500	500	Nikon 40x	7.1±1.1 (n=15)
1700 (in vivo)	-150	200	150	500	200	300	400	200	Olympus 25x	*19.2 ± 3.8 (n=7)

*In vivo experiments were performed with 17-µm diameter TF-CGH spots.

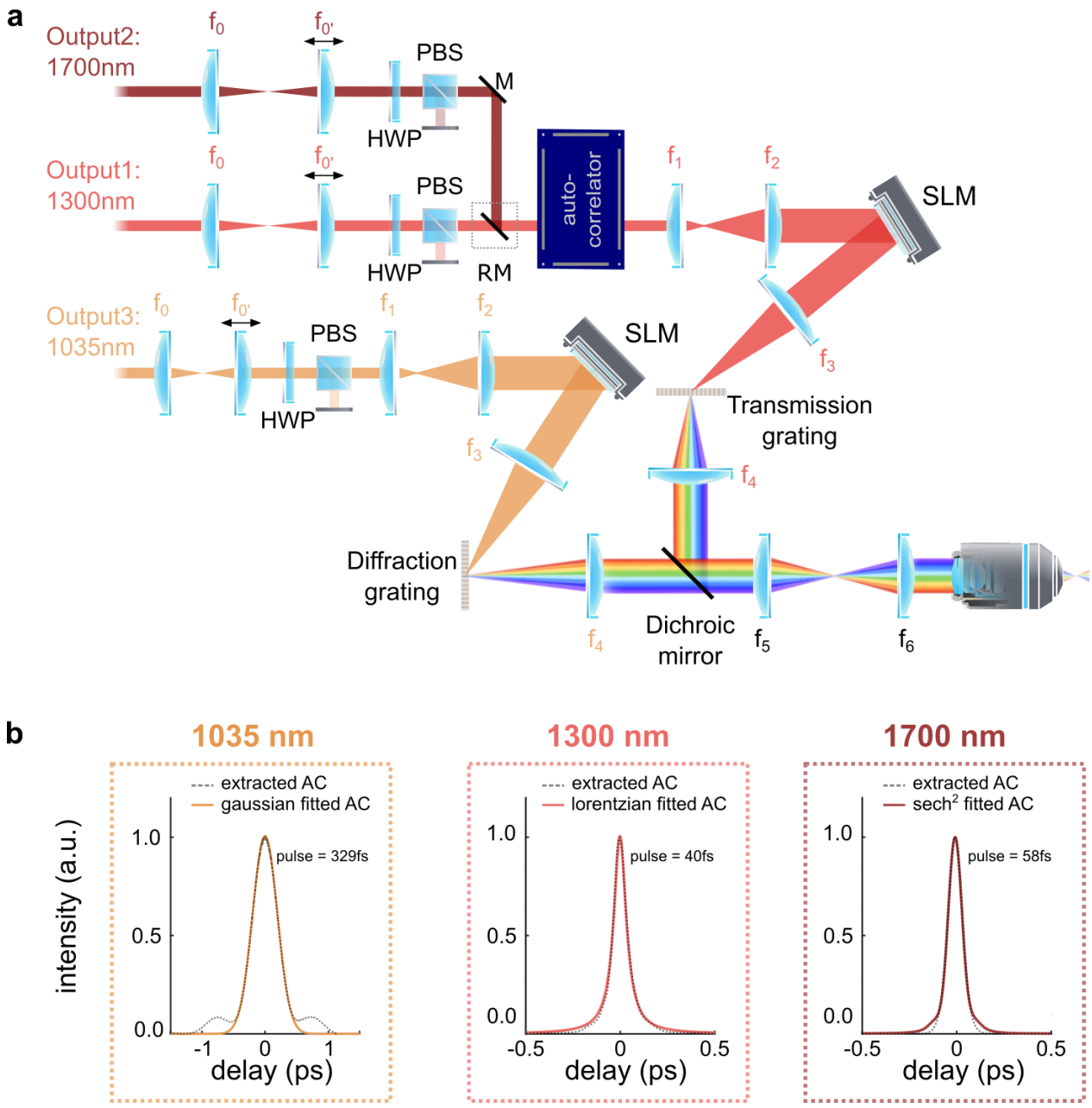

Supplementary Figure 1: Full scheme of the 3P/2P TF-CGH microscope

a Schematic diagram of the optical setup used to perform 2P and 3P optogenetic activation with TF-CGH. A double OPCPA delivers µJ pulses at 1 MHz through three outputs (output 1: 1300 nm, <50 fs, >2.2 µJ, output 2: 1700 nm, <70 fs, >4 µJ and output 3: 1035 nm, <300 fs, >60 µJ). Lenses f_0 and f_0' are used to control the collimation of the beam, in all cases. Power control is performed with a rotating half-wave plate (HWP) and a polarizing beam splitter (PBS) independently for each beam. A removable mirror (RM) is used to direct light from either output 1 or 2 into the 3P microscope optical path. Both 1300-nm and 1700-nm beams go through an autocorrelator (CARPE, APE) for pulse width control. The beams are expanded (f_1 and f_2) to illuminate a phase-only SLM conjugated to the back focal plane of the microscope

objective through the telescope with focal lengths f_3 and f_4, and then a 4*f*-relay telescope with focal lengths f_5 and f_6. A transmission diffraction grating is positioned in a conjugate image plane for temporal focusing. For 2P TF-CGH excitation, the 1035-nm beam after being expanded by f_1 and f_2, illuminates the SLM, which is conjugated to the back focal plane of the objective via the telescopes $f_3 - f_4$ and $f_5 - f_6$. A reflective diffraction grating is placed at the focal plane of the $f_3 - f_4$ telescope for performing temporal focusing. A dichroic mirror combines the 2P and 3P excitation optical paths before the objective. M: mirror. Distances are not in scale. For references of the optical elements and the exact focal lengths of the lenses used, refer to Methods and **Supplementary Table 1**. **b** Intensity autocorrelation traces and fitted laser pulse widths after the objective of the 2P/3P holographic microscope for the 1035 nm, the 1300 nm and the 1700 nm beams. Dashed grey lines are the measured filtered autocorrelation function (ACF) traces, and coloured plain lines are the corresponding fits according to a Gaussian (1035 nm), Lorentzian (1300 nm) and sech^2 (1700 nm) deconvolution.

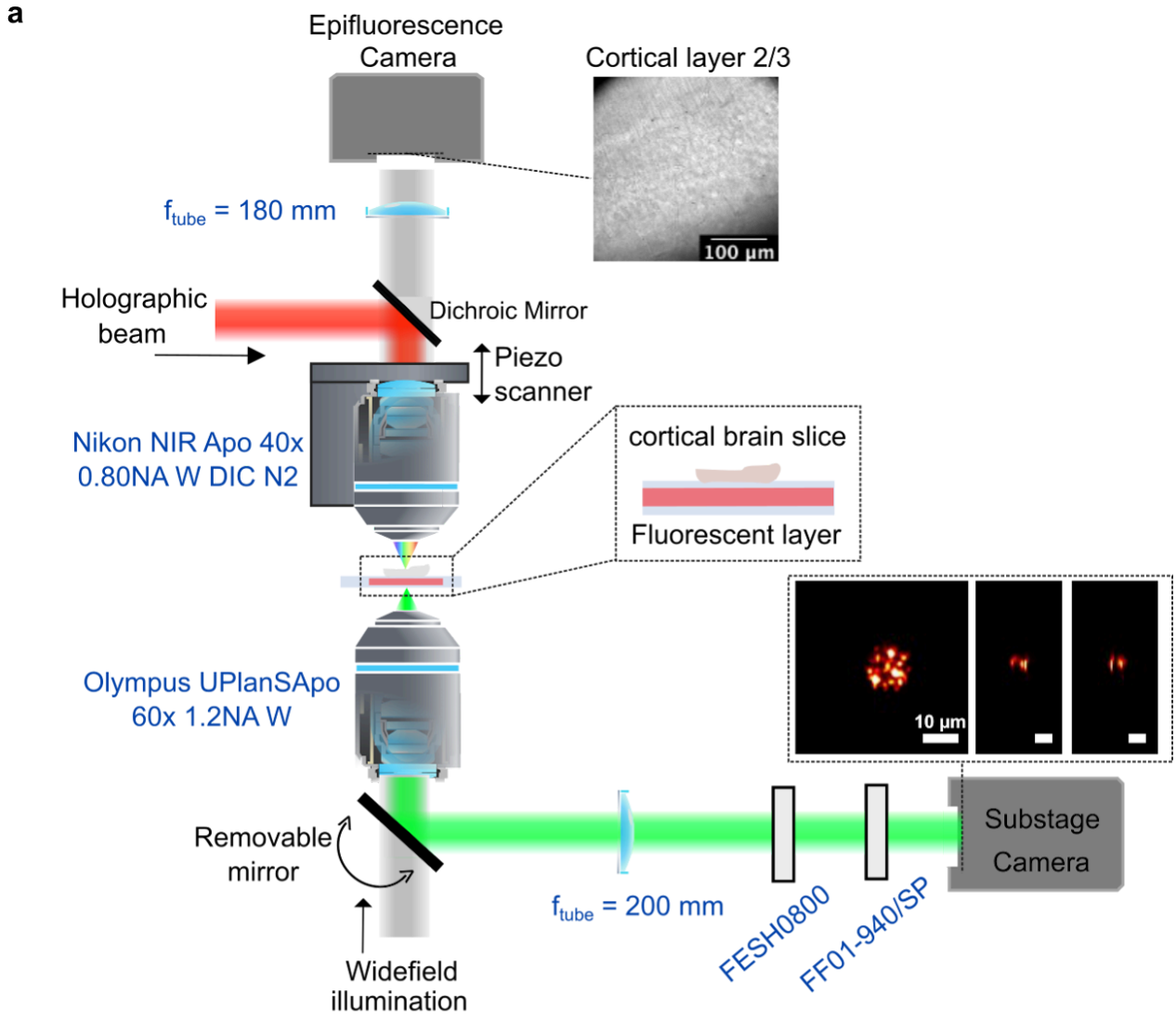
a
Epifluorescence Camera
Cortical layer 2/3
100 µm
f_{tube} = 180 mm
Holographic beam
Dichroic Mirror
Piezo scanner
Nikon NIR Apo 40x 0.80NA W DIC N2
cortical brain slice
Fluorescent layer
10 µm
Olympus UPlanSApo 60x 1.2NA W
Removable mirror
Substage Camera
f_{tube} = 200 mm
FESH0800
FF01-940/SP
Widefield illumination

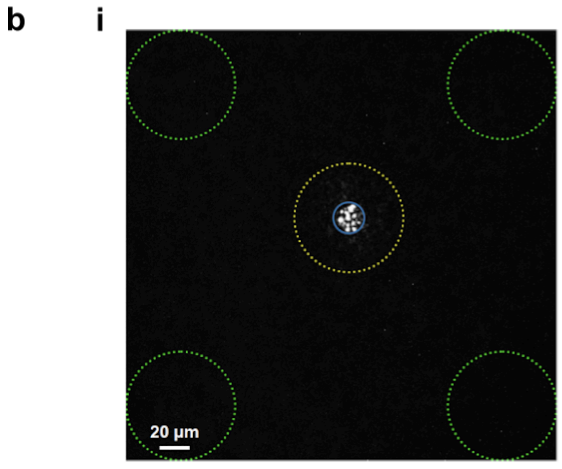
b
i
20 µm

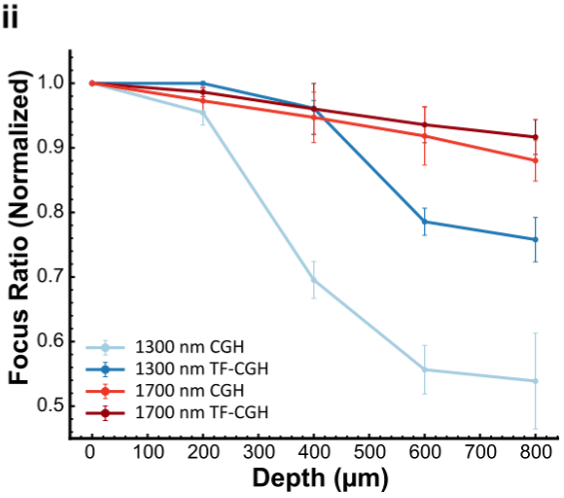
ii
Focus Ratio (Normalized)
1.0
0.9
0.8
0.7
0.6
0.5
1300 nm CGH
1300 nm TF-CGH
1700 nm CGH
1700 nm TF-CGH
0
100
200
300
400
500
600
700
800
Depth (µm)

Supplementary Figure 2: Evaluation of holographic spots in scattering conditions.

a Schematic of the optical setup used for evaluating the holographic beams through scattering tissue. The condenser lens of the microscope was replaced with a high-NA objective (Olympus UPlanSApo 60x, NA1.2) that was collecting the excited fluorescence on the fluorescent thin film (rhodamine or Qdot605 layer) and imaging this to the substage camera, similarly to the experimental method used in (Bègue et al., 2013). Widefield illumination of the sample was possible both from the bottom and the side view for observing the position of the fixed brain slices in the epi-camera detection. Measurements were performed in layer 2-3 of the mouse cortex on fixed brain slices. Holographic excitation was performed through a 40x, 0.8 NA objective (Nikon NIR Apo 40x/0.80W DIC N2). **b** Definition of regions of interest (ROIs) and Focus Ratio across tissue thickness. (i) Example CGH image showing the ROIs used for analysis: the signal ROI (blue; radius R) centred on the main focus; the context ROI (yellow; radius $3.5R$); and the background ROIs (green) positioned in the image corners. (ii) Normalized Focus Ratio measured for the 0 µm reference condition and for fixed brain slices of 200, 400, 600, and 800 µm thickness. Coloured lines correspond to the experimental conditions indicated in the legend. The Focus Ratio is defined as described in Methods (Equation 4). All values are normalized such that the 0 µm condition equals 1.

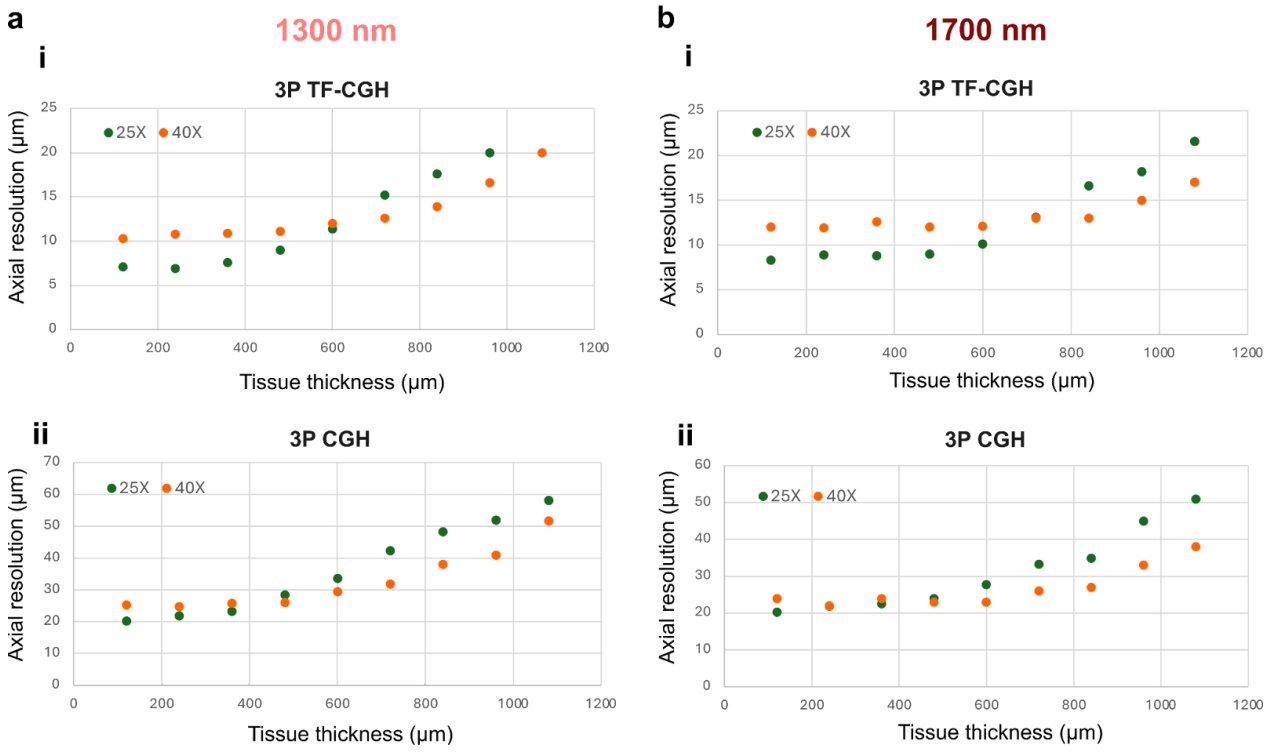

Supplementary Figure 3: Theoretical simulations of holographic beam propagation through scattering media.

Theoretical simulations of 15-µm diameter TF-CGH (**i**) and CGH (**ii**) spots' beam propagation through tissue. The FWHM of the axial intensity distribution (axial resolution) of the spots is plotted as a function of tissue thickness (0-1100 µm) at 1300 nm (**a**) and 1700 nm (**b**), for the two different objectives used in this work, the 40×, 0.8 NA and the 25×, 1.0 NA. We observed a similar behaviour for both objectives with increasing tissue thickness. The axial FWHM was broader for the 40× objective at shallow depths, consistent with its lower numerical aperture, and was therefore less affected by increasing imaging depth.

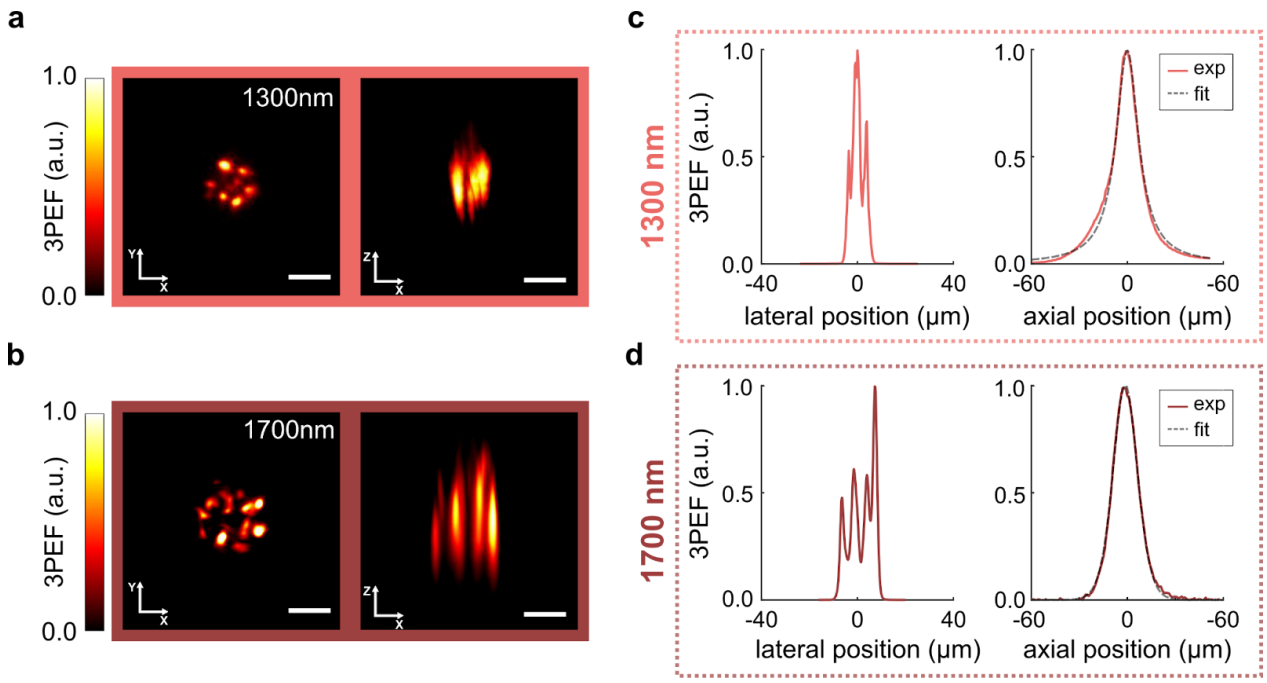

Supplementary Figure 4: Optical performances of the 3P holographic microscope with the Olympus 25x XLPLN25XSVMP2, NA 1.0 objective.

a-b Representative lateral and axial profiles of 3P excited fluorescence (3PEF) generated on a thin rhodamine-6G layer with a 12-µm-diameter TF-CGH spot at 1300 nm (**a**) and a 16-µm-diameter TF-CGH spot at 1700 nm (**b**). Scale bars represent 10 µm. **c-d** Representative lateral and axial profiles of 3P excited fluorescence generated on the rhodamine-6G layer with a 12-µm-diameter TF-CGH spot at 1300 nm (**c**) and a 16-µm-diameter TF-CGH spot at 1700 nm (**d**). In the axial profile, 'exp' refers to experimental data and 'fit' to the corresponding Lorentzian fit (axial FWHM of 16±4 µm, n=10 for 1300nm (**c**) axial FWHM of 18.1±1.7 µm, n=10 for 1700nm (**d**)).

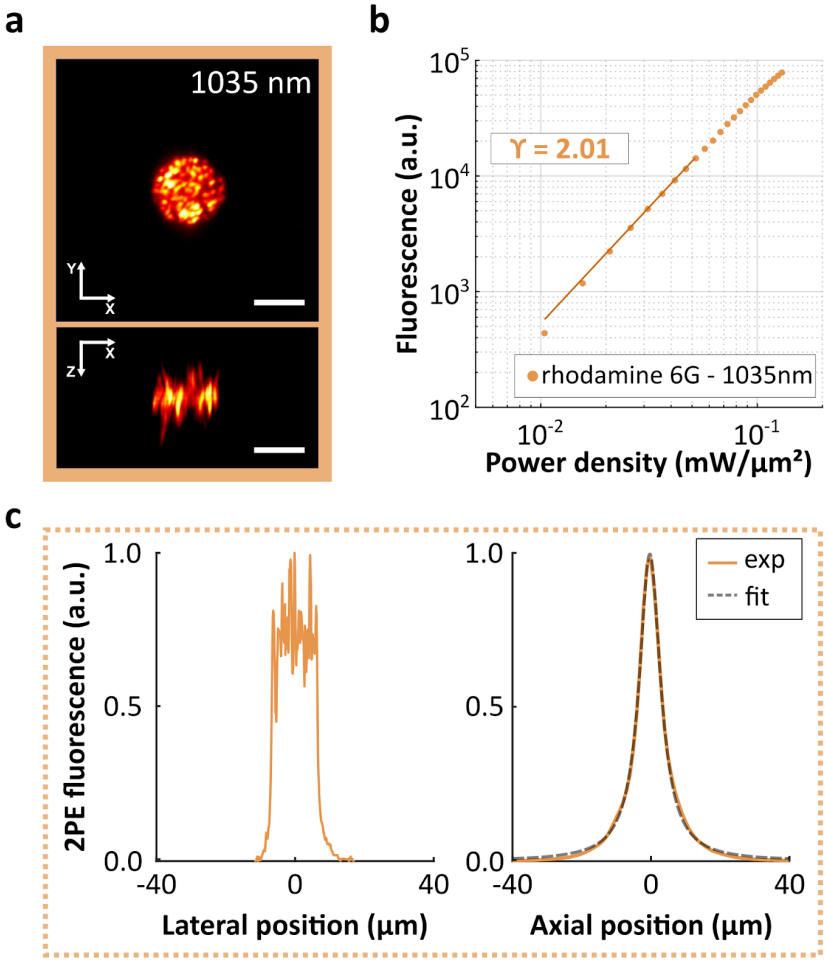

Supplementary Figure 5: Optical performances of the 2P holographic microscope.

a Representative lateral and axial profiles of 2P excited fluorescence generated with a 15-µm-diameter TF-CGH spot at 1035 nm. Scale bars represent 10 µm. **b** Power dependence of the fluorescence excited on a rhodamine-6G spin-coated layer under excitation at 1035 nm with a TF-CGH beam. The line is a linear fit to the log-transformed data (yellow dots). The slope (ϒ) and coefficient of determination (R^2) value of the linear fit to log-transformed data are shown. **c** Representative lateral and axial profiles of 2P excited fluorescence generated with 15-µm-diameter TF-CGH spots at 1035 nm on the rhodamine-6G layer, and collected using a widefield detection axis equipped with a detection objective and a sCMOS camera (see Methods). In the axial profile, 'exp' refers to experimental data and 'fit' to the corresponding Lorentzian fit (axial FWHM of 7.8±0.7 µm, n=7). Excitation objective: Nikon NIR Apo 40x/0.80W DIC N2 objective.

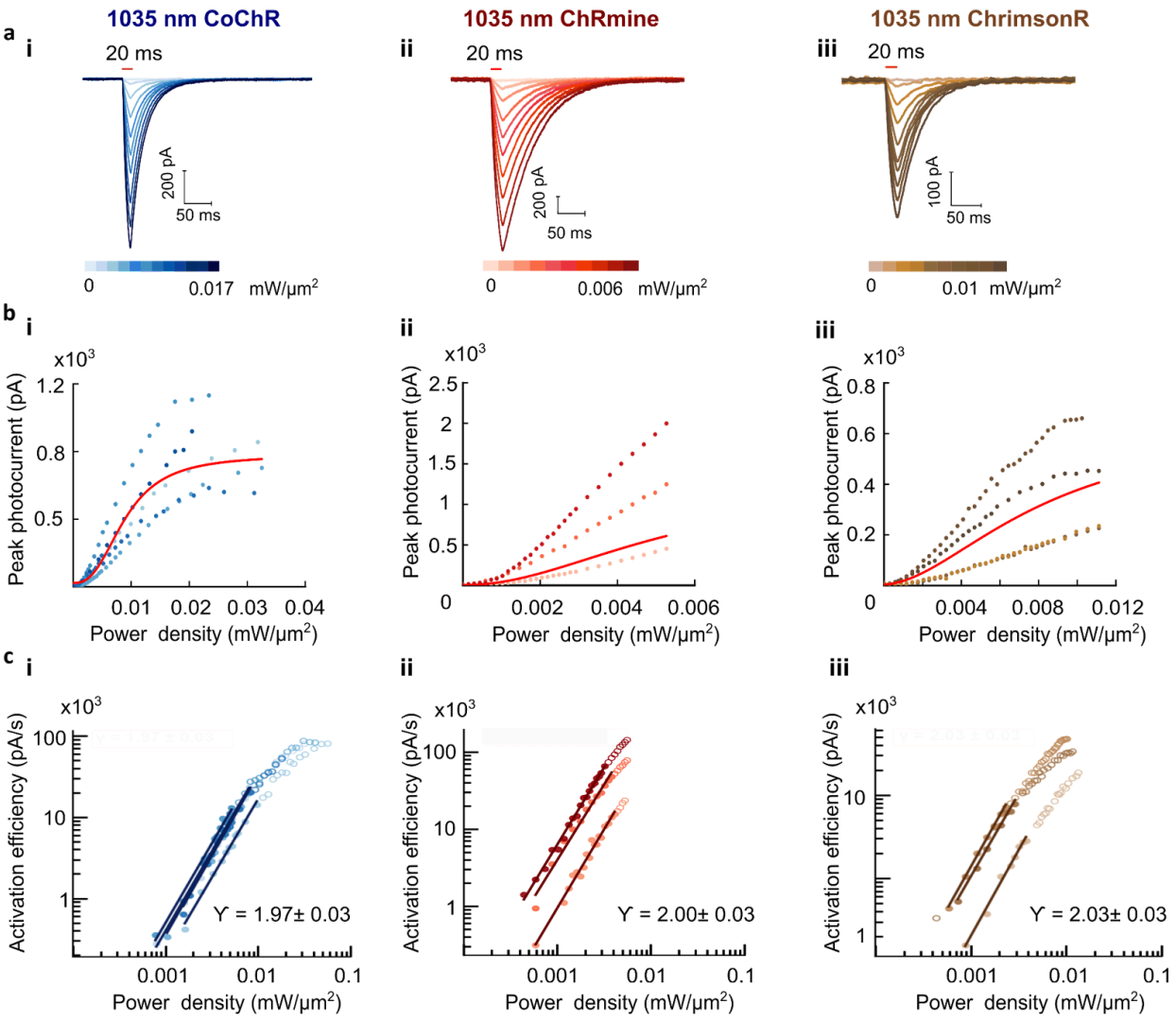

Supplementary Figure 6: 2P TF-CGH excitation of neurons expressing excitatory opsins.

a Representative whole-cell photocurrents recorded from neurons expressing **(i)** CoChR, **(ii)** ChRmine, and **(iii)** ChrimsonR under 1035 nm illumination at increasing power density. **b** Power curves showing the relationship between photocurrent amplitude and illumination power density for **(i)** CoChR (n=5), **(ii)** ChRmine (n=3), and **(iii)** ChrimsonR (n=4). Points of the same colour represent individual cells, and solid red lines are the logistic fit of average photocurrents. **c** Activation efficiency as a function of excitation power density plotted on a log-log scale. The slope (Ɣ; mean ± SD) is derived from linear fits (solid lines) of the titration curves for **(i)** CoChR (n = 6), **(ii)** ChRmine (n = 3), and **(iii)** ChrimsonR (n = 4). Points of the same colour represent individual cells. Excitation objective: Olympus 25× XLPLN25XSVMP2, NA 1.0.

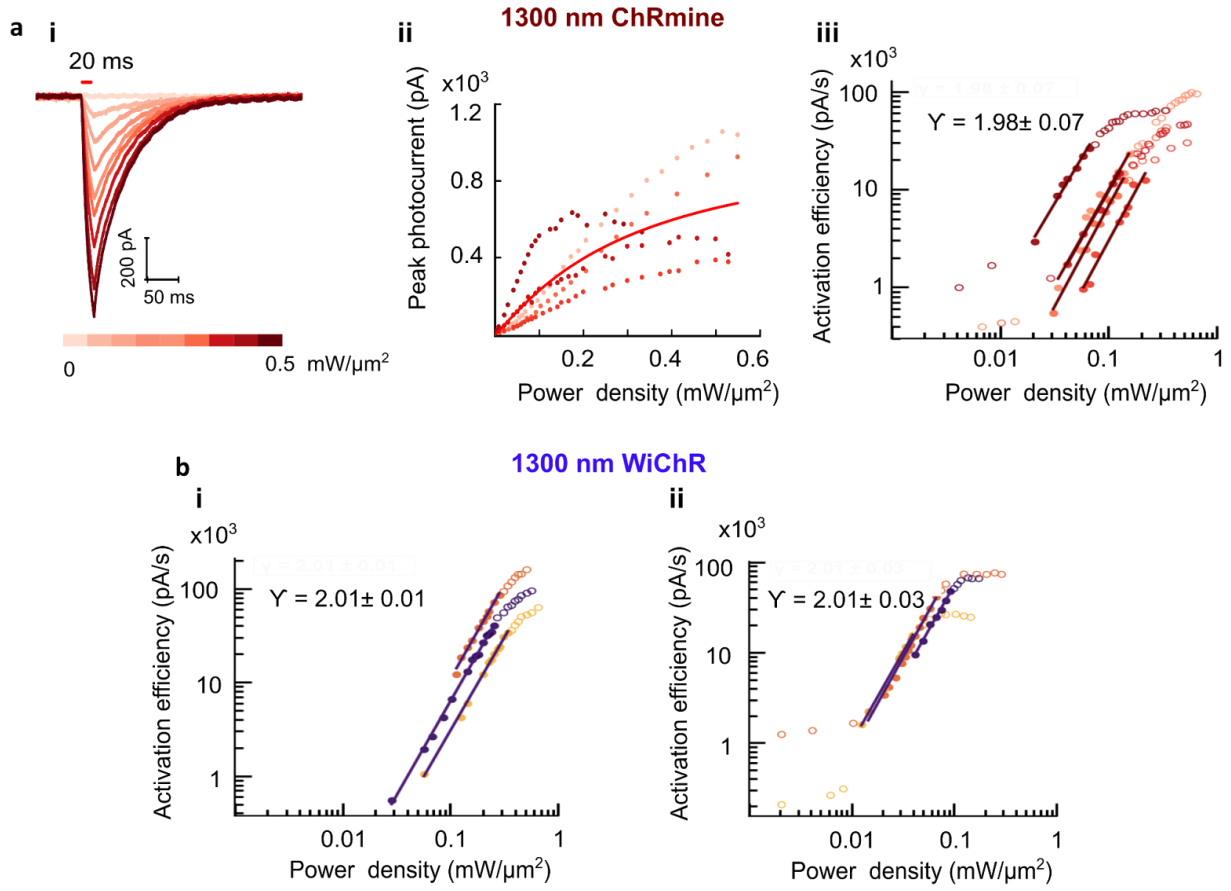

Supplementary Figure 7: ChRmine and WiChR photoactivation under 1300-nm TF-CGH excitation.

a (i) Representative whole-cell photocurrents recorded from neurons expressing ChRmine, under 1300 nm illumination at increasing power density. **(ii)** Power curves showing the relationship between photocurrent amplitude and illumination power density. Points of the same colour represent individual cells, and solid red lines are the logistic fit of average photocurrents. **(iii)** Activation efficiency as a function of excitation power density plotted on a log–log scale (n = 6). **b** Activation efficiency as a function of excitation power density plotted plotted on a log–log scale for **(i)** neurons expressing WiChR (n=3) and **(ii)** CHO cells expressing WiChR (n=3) under 1300 nm illumination. The slope (Ƴ; mean ± SD) is derived from linear fits (solid lines) of the titration curves. Excitation objective, Nikon NIR Apo 40x/0.80W DIC N2.

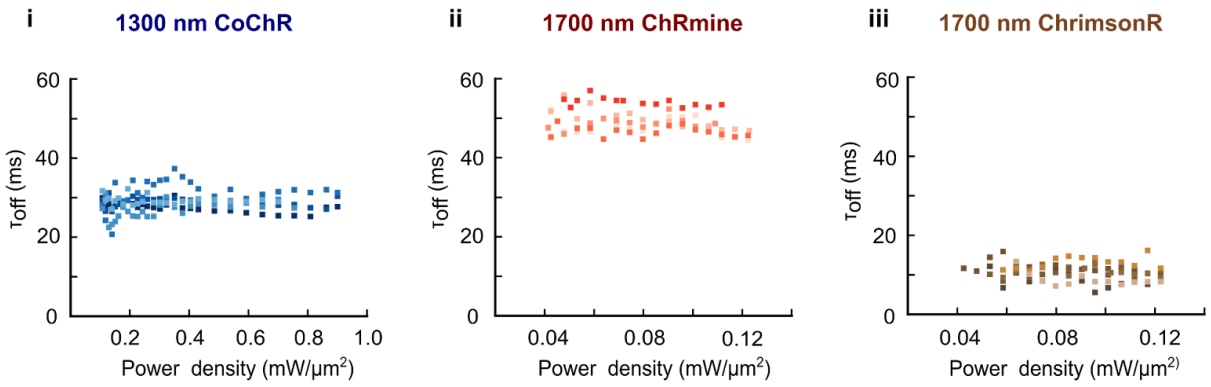

Supplementary Figure 8: Photocurrent kinetics of opsins under 3P and 2P TF-CGH excitation.

a τ_{off} of opsin-mediated photocurrents as a function of 3P TF-CGH stimulation power densities for (**i**) CoChR (1300 nm; n=4), (**ii**) ChRmine (1700 nm; n=5) and (**iii**) ChrimsonR (1700 nm; n=4). Excitation objective, Olympus 25x XLPLN25XSVMP2, NA 1.0.

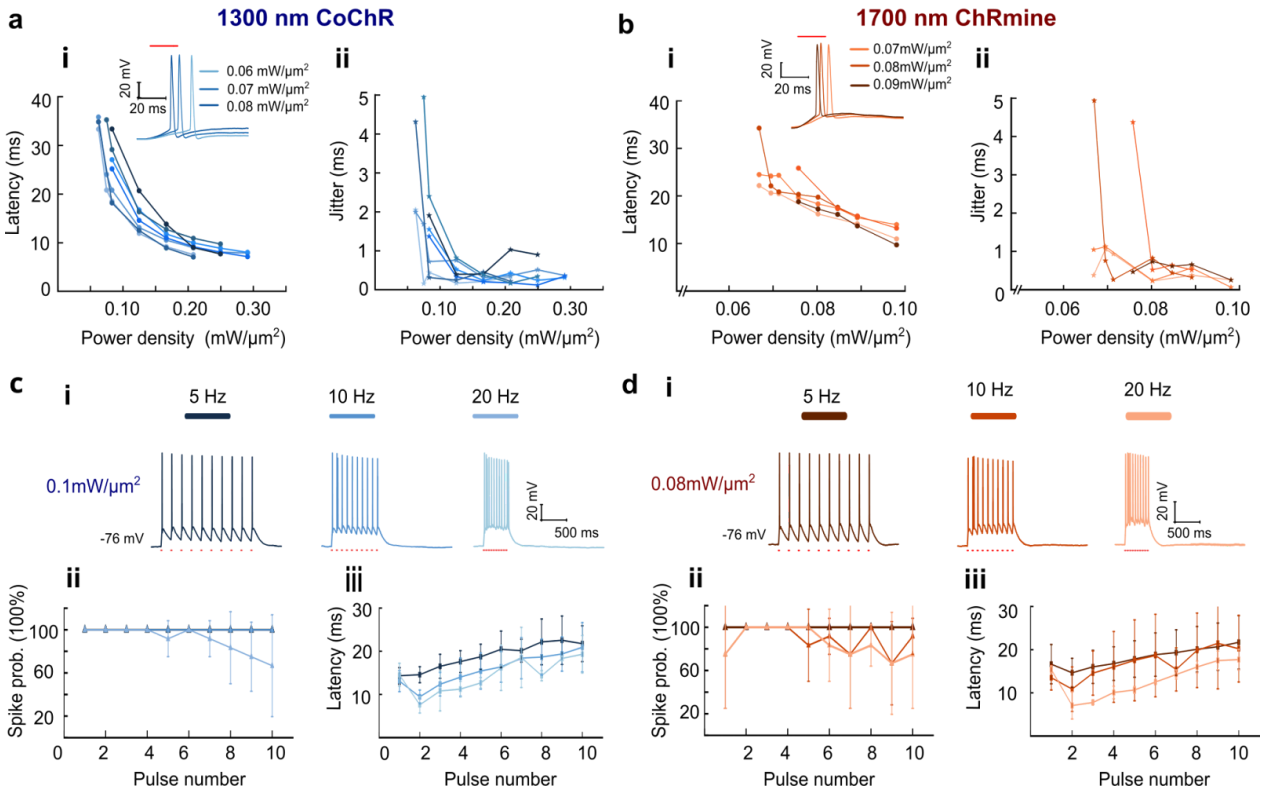

Supplementary Figure 9: 3P light-evoked spiking of neurons expressing CoChR and ChRmine using the Nikon NIR Apo 40x/0.80W DIC N2 objective

a-b (i) AP latencies and (ii) jitter as a function of illumination power density in neurons expressing CoChR (**a**) and ChRmine (**b**) measured after TF-CGH excitation at 1300 nm and 1700 nm, respectively. Connected dots of different colours represent data from the same cell (CoChR, n=7; ChRmine, n= 5). Inset, representative APs generated by different illumination power densities. **c-d** (i) Representative spike trains evoked by 10 photostimulation pulses delivered at 5, 10 and 20 Hz, in neurons expressing CoChR (**c**) and ChRmine (**d**). (ii) Spike probability in relation to pulse order under different power for stimulation at 5, 10 and 20 Hz. (iii) AP latency in relation to pulse order at 5, 10 and 20 Hz under different illumination powers (CoChR, n=4; ChRmine, n= 5).

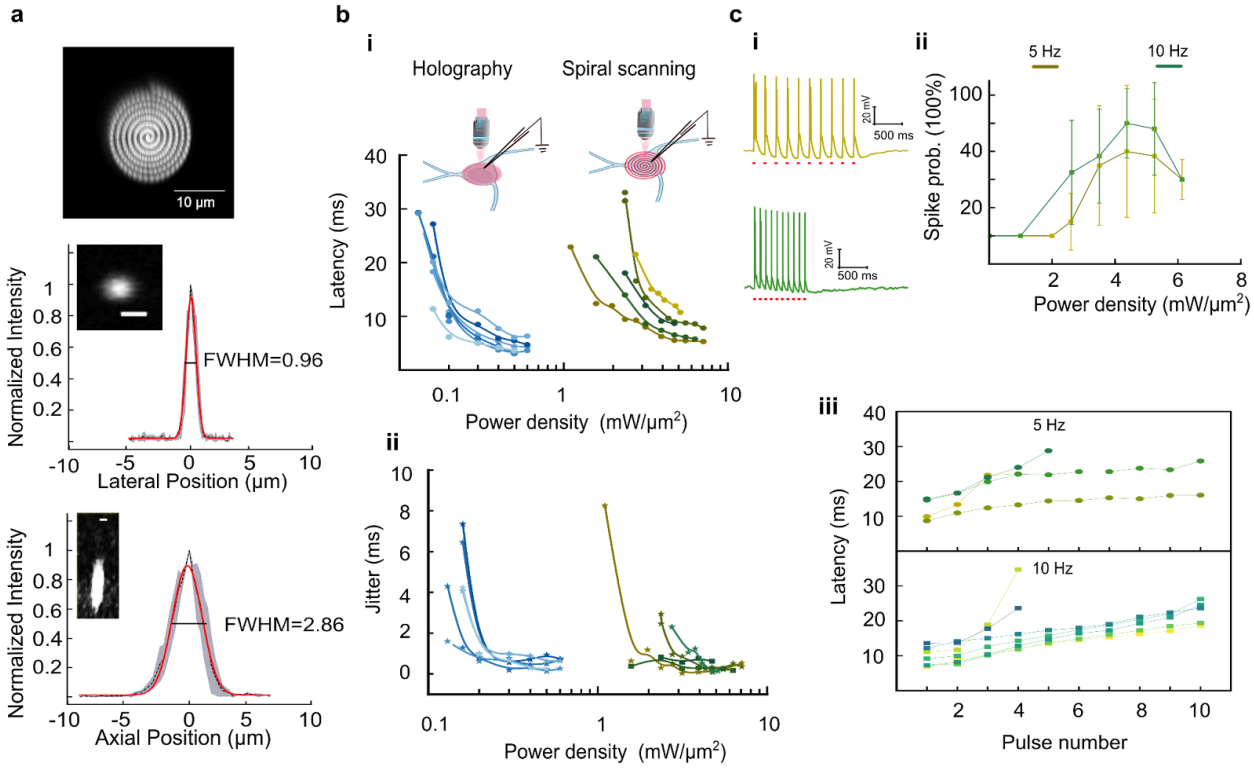

Supplementary Figure 10: 3P optogenetics with spiral illumination in neurons expressing CoChR.

a Fluorescence image showing the spiral scan path (7 revolutions) expanding outward from the cell centre to the boundary. Bottom graphs show the point spread function (PSF) characterization along the *y* and *z* axis. The normalized mean intensity profile (black dashed line) is shown with its variability (±1σ, gray shading) and fitted with a Gaussian model (red solid line). The fit yields a FWHM of 0.96 µm in *y* and 2.86 µm in *z*. The FWHM in *x* was 0.90 µm (plot not shown). Insets show images of the lateral (*x*-*y*) and axial (*y*-*z*) fluorescence intensity of a 200-nm diameter green bead acquired on the PMT (Scale bar: 1µm). **b** (i) AP latencies and (ii) jitter as a function of illumination power density in neurons expressing CoChR following TF-CGH excitation (left, n = 6) and spiral scanning (right, n = 5) at 1300 nm. Data points of the same color represent data from the same cell. **c** (i) Representative spike trains evoked by 3P spiral scanning with stimulation at 5 Hz and 10 Hz. (ii) Spike probability as a function of illumination power density, and (iii) AP latency as a function of pulse order during 5 and 10 Hz stimulation, with the latter extracted at the power densities yielding the maximum number of APs (3.5–6.5 mW/µm²; 10 Hz, n = 6; 5 Hz, n = 4). Excitation objective: Olympus 25× XLPLN25XSVMP2, NA 1.0.

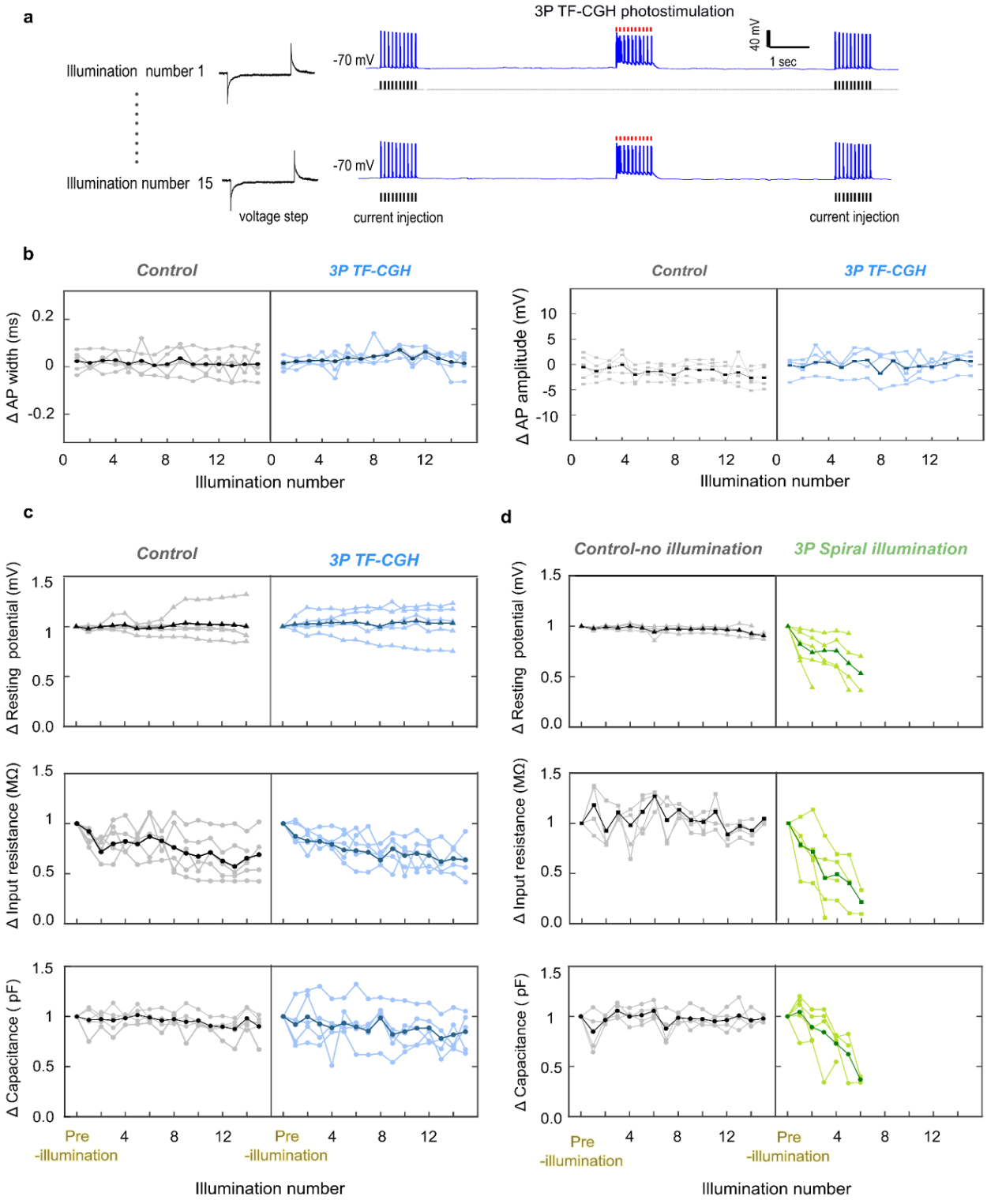
a
3P TF-CGH photostimulation
Illumination number 1
Illumination number 15
-70 mV
-70 mV
40 mV
1 sec
voltage step
current injection
current injection
b
Control
3P TF-CGH
Δ AP width (ms)
Δ AP amplitude (mV)
Illumination number
c
d
Control
3P TF-CGH
Control-no illumination
3P Spiral illumination
Δ Resting potential (mV)
Δ Input resistance (MΩ)
Δ Capacitance (pF)
Pre -illumination
Illumination number

Supplementary Figure 11: Evaluation of cell photodamage under 3P TF-CGH illumination and 3P spiral illumination in neurons expressing CoChR at 1300 nm

a Representative recordings illustrating the experimental protocol used to assess photodamage under 3P-TF-CGH illumination. For each stimulation round, a –10 mV voltage step was applied in voltage-clamp to monitor membrane properties, followed by current-clamp recording without holding current to track resting membrane potential. A 10 Hz train of APs was evoked by brief current injection before and after photostimulation to assess AP waveform. Photostimulation trains (10 pulses, 20 ms, 10 Hz) were delivered at 0.06–0.15 mW/µm² and repeated 15 times with 1-min intervals between illumination trains. **b** AP waveform stability during repeated 3P-TF-CGH stimulation. Relative changes in AP amplitude and AP width (normalized to the first illumination round) are measured from electrically evoked APs before and after photostimulation to assess potential photostimulation-induced alterations in intrinsic excitability, while ensuring consistent comparison with control cells. **c** Membrane stability during repeated 3P-TF-CGH stimulation. Relative changes in resting membrane potential, input resistance and membrane capacitance (normalized to the pre-illumination value) are plotted as a function of stimulation round (3P-TF-CGH,n = 6; control, n = 5). Excitation objective: Nikon NIR Apo 40×/0.80 W DIC N2. **d** Membrane stability during repeated 3P spiral scanning. Relative changes in resting membrane potential, input resistance, and membrane capacitance (normalized to the pre-illumination value) are plotted across stimulation rounds. Spiral illumination (4–6 mW/µm²; 10 Hz, 15 ms pulses) was delivered and repeated at 1-min intervals until the patch-clamp recording could no longer be maintained (3P spiral, n = 5; control, n = 4). Excitation objective: Olympus 25× XLPLN25XSVMP2, NA 1.0.

In all plots, connected points represent measurements from individual cells; dark points indicate the mean across cells.

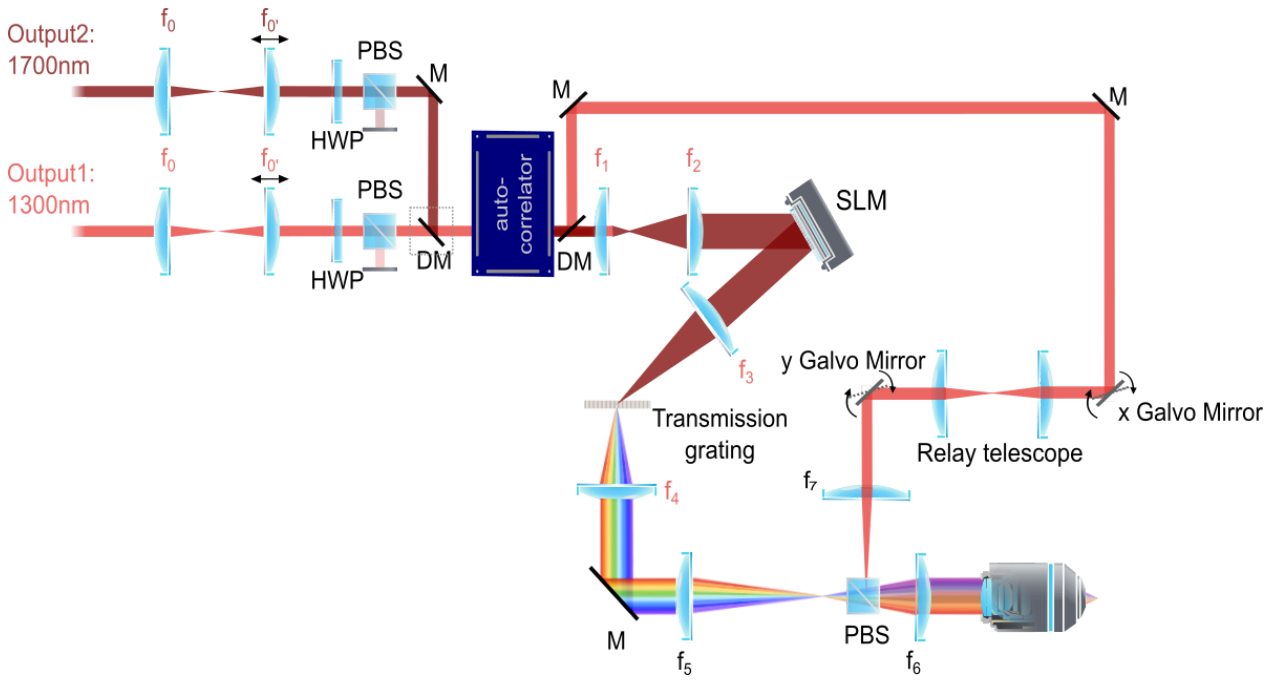

Supplementary Figure 12: Schematic of the optical setup used for the in vivo 3P all-optical experiments.

For all-optical in vivo experiments, output 1 of the OPCPA laser system at 1300 nm was guided through a scanning path with two galvanometric mirrors relayed with a 4-f telescope. A scan lens f_7 and tube lens f_6 magnified the beam to the back aperture of the objective. Tube lens f_6 was shared with the TF-CGH path, built around the 1700 nm beam (output 2 of the OPCPA system) as described previously (see **Supplementary Fig. 1** and Methods). For optical elements references and the focal lengths of the lenses refer to Methods and **Supplementary Table 1**. Distances in the figure are not in scale. HWP: Half-wave plate, PBS: Polarizing beam splitter, DM: Dichroic Mirror, M: Mirror, SLM: Spatial Light Modulator.

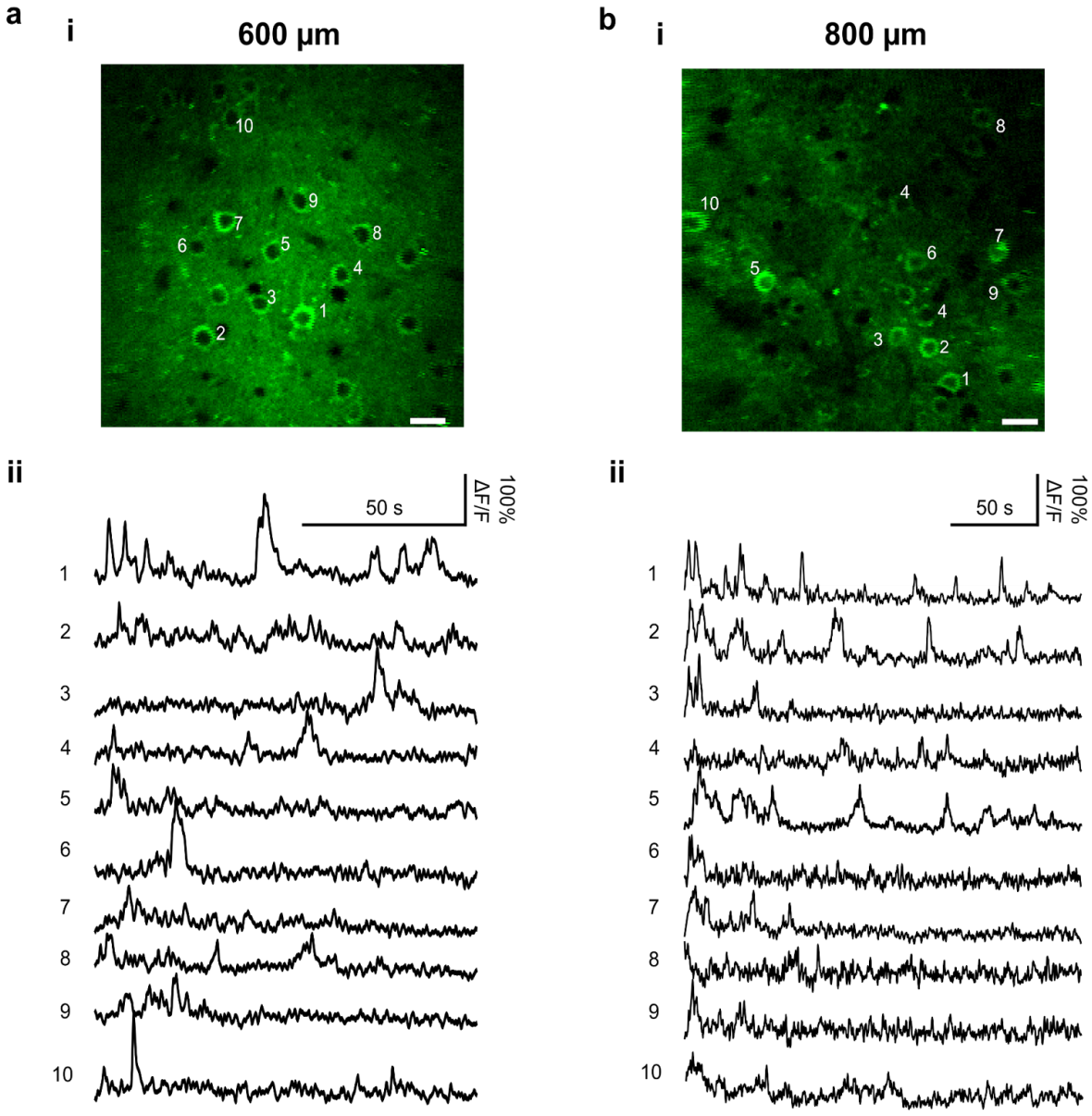

Supplementary Figure 13: Spontaneous neuronal activity under 3P imaging in the awake mouse cortex.

a–b i, Representative average-intensity projection images (green PMT channel; 256 × 256 pixels) of neurons expressing GCaMP6m in the awake mouse cortex, acquired at depths of 600 µm (**a**) and 800 µm (**b**) below the cortical surface. Images are projections of 600 frames acquired at 4.23 Hz using 1300-nm excitation. Scale bar, 20 µm. **ii,** Representative spontaneous calcium activity traces recorded from the corresponding labeled neurons shown in (**i**), at depths of 600 µm (**a**) and 800 µm (**b**), respectively.

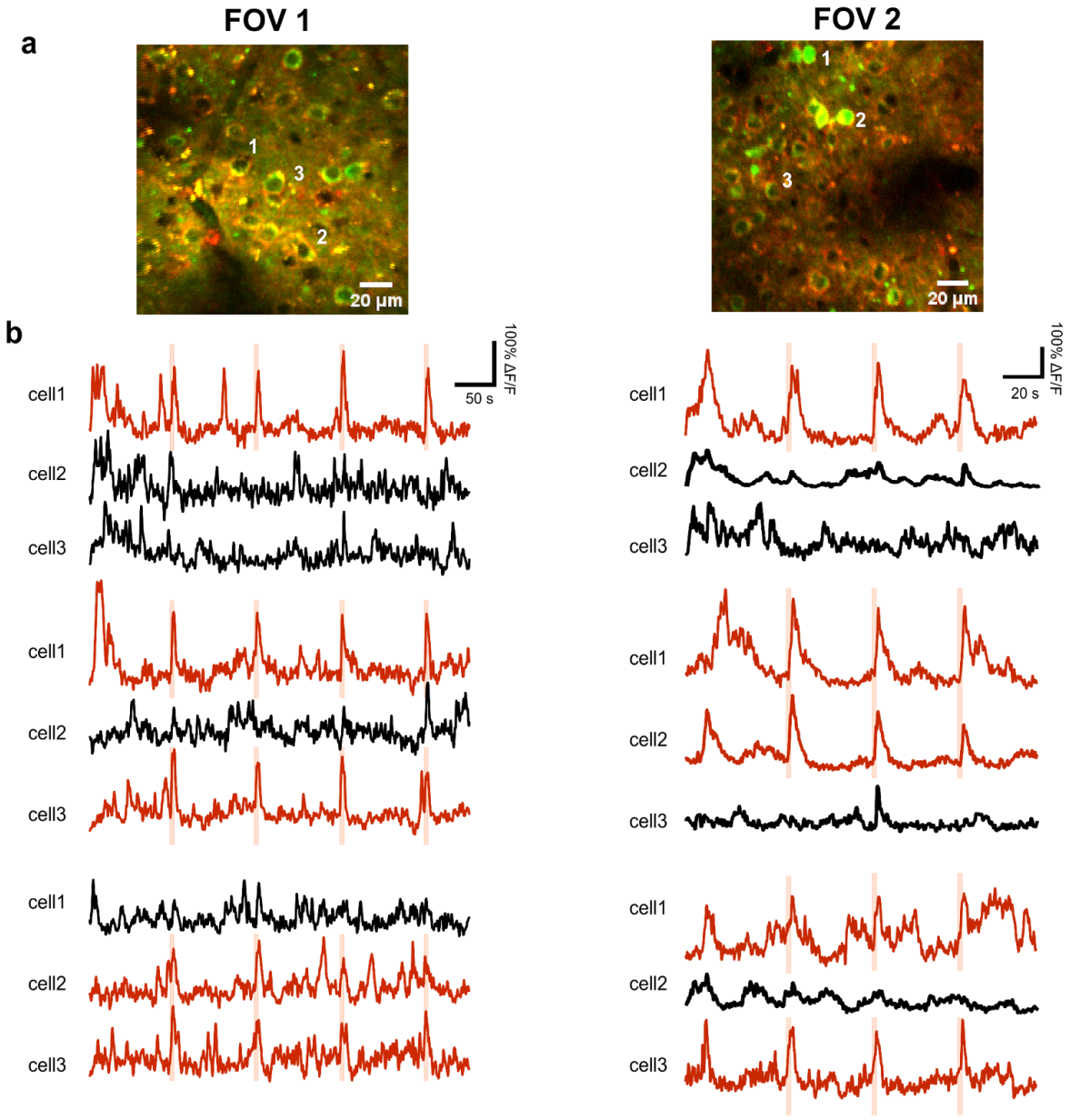

Supplementary Figure 14: All-optical manipulation of neurons in-depth with single-cell resolution.

a Average-intensity projections of 3P-excited fluorescence images of cortical neurons co-expressing GCaMP6m (green) and ChRmine–oScarlet (red) in awake mice, acquired at a depth of 600 µm below the cortical surface in two representative fields of view (FOV) (256 × 256 pixels). Scale bar, 20 µm. **b** Calcium responses of the indicated numbered neurons during targeted photostimulation. Red traces correspond to optogenetically stimulated neurons (1–2 neurons targeted simultaneously per FOV), whereas black traces correspond to non-stimulated neurons. ChRmine-expressing neurons were stimulated using a train of 10 pulses at 10 Hz delivered at 1700 nm, while GCaMP6m fluorescence was imaged at 1300 nm at a frame rate of 4.23 Hz.

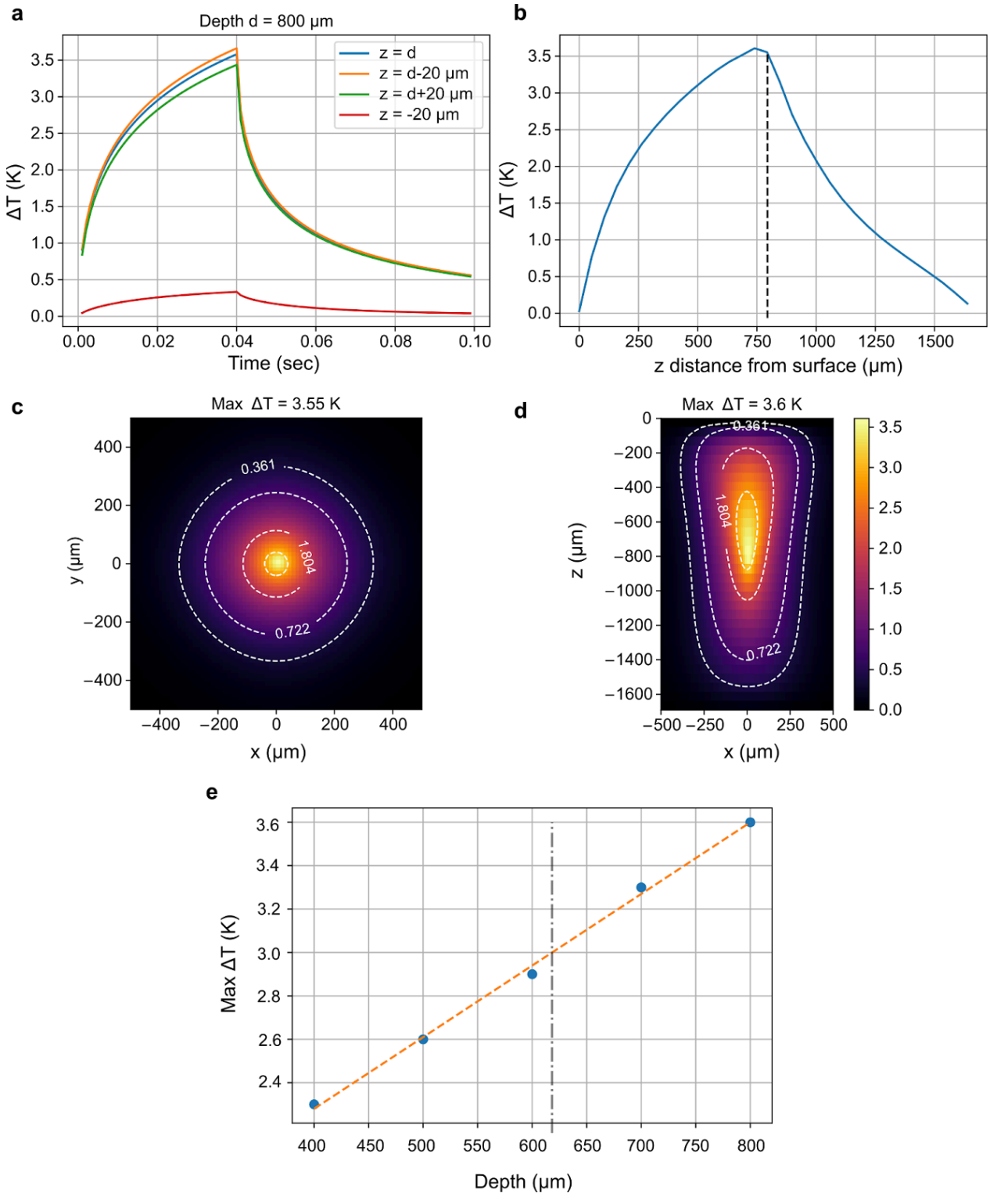
a
Depth d = 800 μm
z = d
z = d-20 μm
z = d+20 μm
z = -20 μm
ΔT (K)
Time (sec)
b
ΔT (K)
z distance from surface (μm)
c
Max ΔT = 3.55 K
0.361
1.804
0.722
y (μm)
x (μm)
d
Max ΔT = 3.6 K
0.361
1.804
0.722
z (μm)
x (μm)
e
Max ΔT (K)
Depth (μm)

Supplementary Figure 15: Simulations of temperature rise *in vivo*.

a Temperature rise (ΔT) over time under *in vivo* illumination conditions used for single-neuron photoactivation at a depth of 800 µm (15 mW at the cell; five 40 ms photostimulation pulses delivered at 10 Hz). ΔT at different depths are shown in distinct colours: blue, focal plane; orange, 20 µm above the focal plane; green, 20 µm below the focal plane; red, 20 µm below the tissue surface (refer to the legend in panel **a**). **b** ΔT over distance from surface for the same conditions simulated in **a** (blue curve). The dashed black line indicates the position of the focal plane of the excitation spot. **c** Transverse (*x*–*y*) ΔT distribution at the focal plane of the excitation of a neuron targeted at 800 µm, as described in **a**. **d** Longitudinal (*x*–*z*) ΔT distribution along the optical axis. Color scale in **c** and **d** represents the local ΔT in Kelvin, with a maximum temperature increase of ΔT = 3.6 K slightly above the beam focus. White dashed lines denote isothermal contours, i.e. curves of equal temperature increase. **e** Maximum ΔT simulated for single-neuron photoactivation at different depths from 400 to 800 µm, using the same stimulation conditions, as described in **a**. Dashed orange line indicates a linear fit of the data points. We observe that ΔT exceeds locally the 3 K for depths >618 µm (dashed grey line).

Supplementary Video 1: 3P structural imaging of the Tg mouse line Ai228

Three-dimensional z-stack acquired to depths exceeding 800 µm below the cortical surface, showing neurons expressing ChRmine–oScarlet imaged at 1300 nm. Images were collected at 1.04 Hz while excitation power was progressively increased with depth according to equation (7), resulting in an average power of 2.80 ± 0.23 mW at the focal plane. Scale bar, 100 µm.

Supplementary Video 2: Photostimulation of a neuron at 800 µm depth

Field of view acquired at a depth of 800 µm showing neurons co-expressing GCaMP6m (green) and ChRmine–oScarlet (red). The targeted neuron is indicated by a yellow circle. Photostimulation rate: 10 Hz, illumination pulse duration: 40 ms, imaging acquisition rate: 4 Hz. Scale bar, 20 µm.

Supplementary Video 3: Photostimulation of two neurons at 600 µm depth

Field of view acquired at a depth of 600 µm showing neurons co-expressing GCaMP6m (green) and ChRmine–oScarlet (red). Two neurons were targeted, indicated by the yellow circles. Photostimulation rate: 10 Hz, illumination pulse duration: 40 ms, imaging acquisition rate: 4 Hz. Scale bar, 20 µm.